Biochemical and Biophysical Research Communications 410 (2011) 688–691

Contents lists available at ScienceDirect

Biochemical and Biophysical Research Communications

journal homepage: www.elsevier.com/locate/ybbrc

Neuraminidase inhibitor R-125489 – A promising drug for treating influenza virus: Steered molecular dynamics approach

Binh Khanh Mai [a], Mai Suan Li [b,*]

[a] Institute for Computational Science and Technology, 6 Quarter, Linh Trung Ward, Thu Duc District, Ho Chi Minh City, Viet Nam
[b] Institute of Physics, Polish Academy of Sciences, Al. Lotnikow 32/46, 02-668 Warsaw, Poland

ARTICLE INFO

Article history:
Received 29 May 2011
Available online 12 June 2011

Keywords:
Neuraminidase inhibitor
Influenza virus
Steered molecular dynamics
Drug
Rupture force

ABSTRACT

Two neuraminidase inhibitors, oseltamivir and zanamivir, are important drug treatments for influenza. Oseltamivir-resistant mutants of the influenza virus A/H1N1 and A/H5N1 have emerged, necessitating the development of new long-acting antiviral agents. One such agent is a new neuraminidase inhibitor R-125489 and its prodrug CS-8958. An atomic level understanding of the nature of this antiviral agents binding is still missing. We address this gap in our knowledge by applying steered molecular dynamics (SMD) simulations to different subtypes of seasonal and highly pathogenic influenza viruses. We show that, in agreement with experiments, R-125489 binds to neuraminidase more tightly than CS-8958. Based on results obtained by SMD and the molecular mechanics-Poisson–Boltzmann surface area method, we predict that R-125489 can be used to treat not only wild-type but also tamiflu-resistant N294S, H274Y variants of A/H5N1 virus as its binding affinity does not vary much across these systems. The high correlation level between theoretically determined rupture forces and experimental data on binding energies for the large number of systems studied here implies that SMD is a promising tool for drug design.

1. Introduction

In the last century, influenza pandemics occurred in 1918 (Spanish, A/H1N1), 1957 (Asian, A/H2N2) and 1968 (Hong Kong, A/H3N2) killed millions of people [1,2]. Recently, two types of influenza virus, A/H5N1 (avian flu) [3,4] and A/H1N1 (swine flu) [5,6] have occurred and spread all over the world causing death in both people and millions of poultry. For the time being the swine flu A/H1N1 is in a post-pandemic phase, [7] but no one can predict when the next pandemic will occur. Two types of drugs are licensed to treat influenza virus. The first class is a M2 inhibitor (amantadine and rimantadine), [8] which blocks the M2 proton channel of influenza preventing the virus from being able to uncoat [9]. These drugs are ineffective against influenza B [9,10] and a number of amantadine-resistant cases have been reported [11]. The second class of drugs involves the neuraminidase (NA) inhibitors oseltamivir (Tamiflu) and zanamivir (Relenza), which are able to block the release of new virons from an infected cell [12]. These inhibitors are often effective against both influenza A and B virus, [10] but some strains of avian A/H5N1 [13,14] and swine A/H1N1 influenza [15–17] are resistant to Tamiflu. Thus, it is vital to design a drug that is capable of treating both influenza A and B as well as their mutants. Furthermore, Tamiflu must be administrated twice daily for 5 days. An important goal is to produce antiviral agents that act longer than existing drugs.

In order to achieve these two goals (efficacy in treatment and long action), experiments have been carried out on the compound R-125489 and its prodrug, CS-8958 [18–22]. These ligands seem to be the most promising leads due to its long-acting activity and good binding affinity to NA of both types A and B, and their variants. Despite their importance understanding the mode of action of these drugs has yet to be considered theoretically. One of our goals is to explore the binding mechanisms of new leads to influenza A and B targets using the steered molecular dynamics (SMD) method [23]. In agreement with experiments, [18–22] we have shown that R-125489 displays higher binding affinity than CS-8958. The reason behind this difference lies in the repulsion between the long "tail" of CS-8958, which contains 7 aliphatic carbons, and the polar residues of the receptor. Using density functional theory we have shown that the equilibrium free energy of R-125489 is lower than CS-8958, which explains why CS-8958 is easily metabolized to R-125489 in the lungs.

Our SMD simulations reveal that the rupture forces and binding affinities of R-125489 are almost the same for wild-type (WT) and

Abbreviations: NA, neuraminidase; SMD, steered molecular dynamics; MM-PBSA, molecular mechanics-Poisson–Boltzmann surface area; vdW, van der Waals; HB, hydrogen bond; RMSD, root mean square displacement; WT, wild-type.

* Corresponding author. Fax: +48 22 8430926.
E-mail address: masli@ifpan.edu.pl (M.S. Li).

0006-291X/$ - see front matter © 2011 Elsevier Inc. All rights reserved.
doi:10.1016/j.bbrc.2011.06.057

mutants N294S and H274Y of A/H5N1. Based on this we predict that, in contrast to Tamiflu, this ligand is good in treating not only WT but also tamiflu-resistant mutants of A/H5N1 influenza virus.

SMD is a promising tool for designing drugs [24,25]. However, previous SMD studies in this area have utilized a limited experimental data base. Therefore, from a methodological perspective, it is important to further validate SMD simulation results through the comparison with a larger set of experimental data. SMD is beneficial because it is computationally much less expensive compared to standard methods for estimating ligand binding affinities [25]. In the present Communication, we show that rupture forces that characterize the stability of receptor–ligand complexes are highly correlated with binding energies experimentally collected for 24 systems [18–22]. Since this data set is much larger than the previous ones, [24,25] our findings strongly support that SMD is a powerful tool for drug design.

2. Materials and methods

2.1. Set of receptor–ligand complexes

Three-dimensional structures of R-125489 and CS-8958 (Fig. S1 in Supporting information (SI)) were built and optimized with the help of Gabedit-2.2.12 software [26]. Atomic types, charges and other parameters of these ligands were assigned using parameters of the Gromos force field 43a1 [27]. Hydrogen atoms were added by the Dundee PRODRG2.5 Server (beta) [28] with the same force field.

Crystal structures of NAs including A/H1N1, A/H5N1, A/H2N2, A/H3N2, A/N4, A/N6, A/N8, A/N9 and B, were taken from the Protein Data Bank (PDB ID: 3NSS, 2HTY, 2BAT, 2AEP, 2HTV, 1V0Z, 2HT5, 7NN9, and 3K36, respectively). Only one chain of NAs from dimer and tetramer structures were extracted for simulation. Ca^{2+} ions in the crystal structure were included in the MD simulations. Coordinates of the N294S and H274Y variants of A/H5N1 were taken from structures 3CL2 and 3CL0, respectively, while other mutants of NAs were created with the help of the Mutagenesis module implemented in the PyMOL package (http://pymol.svn.sourceforge.net). Ligands R-125489 and CS-8958 were first docked to each NA by Autodock Vina 1.1.1 package [29] (see SI for more details), and then their configuration in the best docking mode was used to run MD simulations in the GROMACS 4.5.1 suite [30].

2.2. SMD method

For all-atom simulations NA-ligand complexes were placed in water (see Fig. S2 for a typical conformation). The SPC/E water model [27] was been used. Each system contained roughly 13,000 water molecules. After equilibration in the absence of force, the SMD method was applied to pull ligands from NAs in the z-direction [25] (the choice of pulling direction is described in SI) with a constant velocity $v = 0.005$ nm/ps. The ligand experiences a total force $F = k(vt - x)$, where x is the displacement of the pulled atom from its original position and k is the cantilever spring constant that we set to 600 kJ/(mol nm^2). To ensure the robustness of our results four independent trajectories were generated using different random number seeds.

3. Results and discussions

3.1. R-125489 shows higher binding affinity than CS-8958

Force-extension/time profiles, obtained by pulling two ligands from binding pockets of WT NA of A/H1N1 and B virus, are shown in Fig. 1. The main peak defining the rupture force F_{max} is located away from the initial cantilever position at Δz, which depends on the system under consideration. Before reaching the maximum total force, F increases almost linearly with Δz. After the maxima in this profile the behavior becomes more complicated with the appearance of minor peaks that are irrelevant to the stability of the system. One can show that the main peak occurs due to abrupt change of not only the number of hydrogen bonds (HBs) but also the Coulomb and van der Waals (vdW) interaction between the ligand and residues in the 150-loop [25]. The average number of HBs between R-125489 and A/H1N1 NA is about 2.12 while this number is reduced to 1.34 if it binds to type B NA (Fig. S4). Besides the repulsive interaction between the oxygen atom in the amide group and the carboxyl group of residue Glu277 in both systems, in the type B complex there exists the repulsive interaction between two carboxyl group of R-125489 and Asp150 (Fig. S5). Taken together, R-125489 binds to A/H1N1 NA more tightly compared to type B NA. For both targets the rupture force F_{max} of R-125489 is higher than CS-8958 (Fig. 1). This also holds for the other receptors we studied (Fig. 2 and Table S1 in SI) as the correlation between the experimentally determined binding free energies and F_{max} is very high ($R = 0.97$). Thus, our results are consistent with experiments [18] that show that CS-8958 does not bind as tightly as R-125489 because it can be pulled out from the active pocket by lower external forces. The reason behind this is that CS-8958 has a very long "tail" with 7 aliphatic carbons and this steric constraint does not allow it to be easily accommodated within the binding site. In addition, the vdW repulsion between polar residues of the receptor and CS-8958 tail favors the ligand location near the active pocket mouth making it easily exposed to the environment even under a low applied force.

In an acidic environment the long tail of CS-8958 is reduced as an ester group is replaced by a hydroxyl group or an acceptor group is transformed into the donor group. In the SI we show that in this situation the free energy of binding of R-125489 is lower than that of CS-8958, having a barrier $\Delta G = G(\text{CS-8958}) - G(\text{R-125489}) \approx 4.47$ kcal/mol. Consequently, CS-8958 easily adopts its active form in R-125489 with much higher binding affinity. In other words,

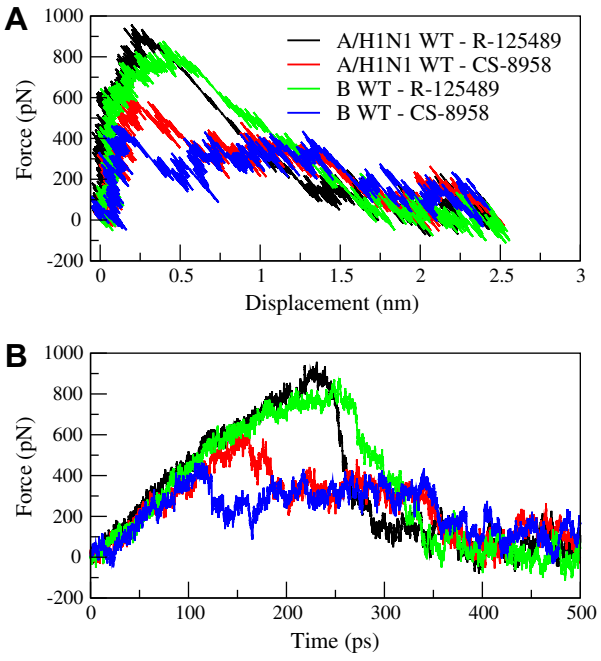

Fig. 1. Shown are force-extension (A) and force–time (B) profiles, obtained by pulling R-125489 and CS-8958 from WT of NA of A/H5N1 and influenza virus B. The external force is applied along the z-direction and pulling speed $v = 0.005$ nm/ps.

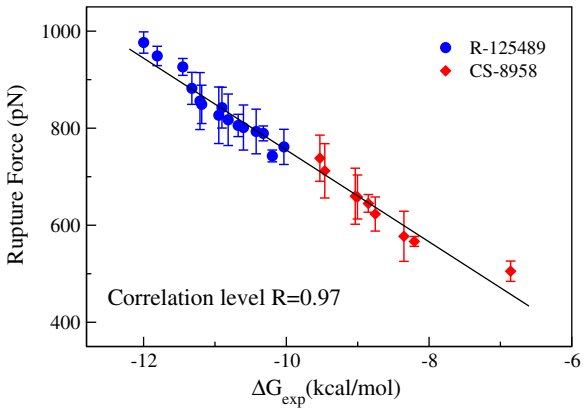

Fig. 2. Correlation between rupture forces and experiment binding energies of R-125489 and CS-8958 to NAs of influenza virus [18]. Results for F_{max} are averaged over 4 pulling trajectories. The linear fit is $y = -191.103–94.611x$ with a correlation level $R = 0.97$.

the change in CS-8958 conformation reduces the steric effect and hydroxyl group can interact with polar residues in the active site leading to an increase in the binding affinity of R-125489 to all NAs. We note that intranasally administrated CS-8958 is quickly metabolized to R-125489 in the lungs and can be retained as a metabolite for a long time [18] (remember that intranasally administrated R-125489 is quickly removed from lung). This makes it possible for R-125489 to be used as a long-acting drug.

3.2. SMD is a promising tool for drug design

It was recently demonstrated that SMD is as good as the molecular mechanics-Poisson–Boltzmann surface area (MM-PBSA) method [31] in predicting the binding affinity of ligands to A/H1N1 and A/H5N1 NA targets [25]. If one uses, for instance, a pulling speed $v = 0.005$ nm/ps, then SMD is computationally about 30-fold faster than MM-PBSA suggesting its great potential for drug design. Because MM-PBSA involves a number of approximations (e.g., water is treated as a continuum environment, snapshots collected in MD runs for receptor–ligand complex are also used to estimate free energies of free subsystems, etc.), the good agreement between results obtained by two methods cannot be used as the sole criterion to justify the SMD approach. The best criterion is the direct comparison with experimental results. In previous studies [24,25] the good correlation between F_{max} values and experimental free energies was obtained only for 5 systems, the study of larger data sets is therefore highly desirable. Here, we have obtained excellent correlation between SMD results and experiment [18] for a much larger data set of 24 systems (Fig. 2). Therefore, our present study strongly supports SMD as a very promising for drug design. The main advantage of SMD is that it is computationally less expensive compared to MM-PBSA, but much more accurate compared to the docking method. In fact, using Vina 1.1.1 package29 for docking we have obtained binding energies which do not correlate with experimental results for the same set of 24 systems (see SI and Fig. S7). This again shows that SMD is superior to the docking approach in estimating the binding affinities of R-125489 and CS-8958.

3.3. R-125489 is good for treating not only A/H5N1 but also its mutants

It is well known that Tamiflu is susceptible to mutations of A/H5N1 [32] (see also Table 2). For N294S and H274Y mutants, for instance, their inhibitory activity are reduced by about 200- and 700-fold compared to WT, respectively. This observation has been also confirmed by our earlier SMD calculations [25] showing that the rupture forces for these mutants are considerably lower than WT (Table 1). The question we ask is if R-125489 is sensitive to mutations of A/H5N1 NA. In order to answer this question we have performed SMD simulations which show that the rupture force varies little among WT and mutants (Fig. S8). The difference in F_{max} between WT and the mutants is about 27 and 40 pN for N294S and H274Y, respectively. However, such a minor difference vanishes considering the error bars in these calculated averages (Table 1). Therefore, we predict that together with WT, N294S and H274Y mutants of A/H5N1 do not show resistance to R-125489 making it efficient for treating not only WT but also Tamiflu resistant mutants of influenza virus. Our prediction is qualitatively supported by the experiments of Kiso et al. [19] who have shown that R-125489 displays almost the same inhibition ability for WT and mutants of VN1203 and HN30408. In fact, using their data on CI50 one obtains $\Delta G_{exp} \approx -13.11$, -11.91 and -12.15 kcal/mol for WT, N294S and H274Y of VN1203, respectively. This implies that the binding of R-125489 is insensitive to mutations.

It should be noted that Zanamivir is also insensitive to mutants of A/H5N119 because the binding energy of WT differs from mutants by an amount less than 1 kcal/mol (Table 1). Our results on rupture forces obtained by the SMD method are in reasonable agreement with this experimental observation as mutations do not alter them much (Fig. S8 and Table 1). The simulations also show that Zanamivir binds to A/H5N1 slightly stronger than Tamiflu, but its binding affinity is comparable with R-125489.

In order to shed more light on the nature of binding of R-125489 to A/H5N1 variants we have carried out 15 ns conventional MD simulations with the Gromos force field 43a1 [27]. As evident from Fig. S9, after 11 ns the system reaches equilibrium as the root mean square displacement (RMSD) becomes saturated. In the equilibrium state (the last 4 ns of MD run), mutants N294S and H274Y have a minor effect on the binding mode of R-125489 as its RMSD remains low (Fig. S10). For both mutants the average value of the equilibrium RMSD is only 0.7 Å. A small variation in R-125489 structure upon mutation is also seen from Fig. S11 which shows the superposition of its typical structures in the binding site

Table 1
The rupture force F_{max} to pull R-125489 out from the binding pocket of WT, N294S, and H274Y variants of A/H5N1 NA and binding free energies. F_{max} and ΔG are measured in pN and kcal/mol, respectively.

A/H5N1	R-125489		Tamiflu		Zanamivir	
	Rupture Force	ΔG_{MMPBSA}	Rupture Force[a]	ΔG_{exp}[b]	Rupture Force	ΔG_{exp}[c]
WT	926.3 ± 17.4	−27.86	862.9 ± 39.8	−13.03	912.7 ± 26.8	−13.73
H274Y	898.8 ± 27.2	−27.48	754.7 ± 26.8	−10.41	822.4 ± 35.4	−12.55
N294S	885.9 ± 29.5	−25.78	687.9 ± 34.6	−9.71	865.3 ± 36.8	−13.34

[a] Data from our previous study [25].
[b] Data from Collins et al. [32].
[c] Data from Kiso et al. [19].

of WT, N294S and H274Y. This partially explains why R-125489 is not so sensitive to mutations.

Using the MM-PBSA method (see SI for more details) and snapshots collected at equilibrium we have estimated the binding free energy of R-125489 to the WT and mutants (Table 1). Overall, the electrostatic interactions play a more important role than the vdW interactions (Table S2). Due to the lack of interactions between Asn294, Tyr347 and carboxyl group of ligand, the average number of HBs formed by R-125489 and receptor is 4.0, 2.7 and 2.3 for WT, H274Y and N294S, respectively (Fig. S12). This makes binding of R-125489 to mutants a bit softer compared to WT. Moreover, due to a small contribution of the vdW interaction (Table 1), H274Y is less stable than others. Thus, both MM-PBSA and SMD methods support ranking WT → N294S → H274Y (Table 1) in terms of their binding affinity for R-125489.

In conclusion, we have demonstrated that, in accord with experiments, [18] R-125489 binds to influenza virus more tightly than CS-8958. We predict that R-125489 can bind not only WT but also tamiflu-resistant mutants of A/H5N1. It would be very interesting to check this prediction in vitro as well as in vivo. The good correlation between theoretically determined rupture forces and a large experimental data set of binding free energies further validates SMD as a promising tool for drug design wherein the binding affinity of a ligand can be judged by its rupture force upon pulling it from the active site.

Acknowledgment

We are very thankful to E.P. O'Brien Jr for the critical reading of the manuscript. This work was supported by the Department of Science and Technology of the Ho Chi Minh City, Viet Nam and the Ministry of Science and Informatics in Poland (Grant No. 202-204-234).

Appendix A. Supplementary data

Supplementary data associated with this article can be found, in the online version, at doi:10.1016/j.bbrc.2011.06.057.

References

[1] P. Palese, Influenza: old and new threats, Nat. Med. 10 (2004) S82–S87.
[2] Y.-C. Hsieh, Wu. T-Z, D.-P. Liu, P.-L. Shao, L.-Y. Chang, C.-Y. Lu, C.-Y. Lee, F.-Y. Huang, L.-M. Huang, Influenza pandemics: past, present and future, J. Formos. Med. Assoc. 105 (2006) 1–6.
[3] N.M. Ferguson, C. Fraser, C.A. Donnelly, A.C. Ghani, R.M. Anderson, Public health risk from the avian H5N1 influenza epidemic, Science 304 (2004) 968–969.
[4] H.-L. Yen, R.G. Webster, Pandemic influenza as a current threat, Curr. Top. Microbiol. Immunol. 333 (2009) 3–24.
[5] WHO, Pandemic (H1N1) 2009 briefing note 4. Available from: <http://www.who.int/csr/disease/swineflu/notes/h1n1_situation_20090724/en/index.html>. (Accessed July 24, 2009).
[6] G. Neumann, T. Noda, Y. Kawaoka, Emergence and pandemic potential of swine-origin H1N1 influenza virus, Nature 459 (2009) 931–939.
[7] WHO, H1N1 in post-pandemic period. Available from: <http://www.who.int/mediacentre/news/statements/2010/h1n1_vpc_20100810/en/index.html>. (Accessed August 10, 2010).
[8] A.J. Hay, A.J. Wolstenholme, J.J. Skehel, M.H. Smith, The molecular basis of the specific anti-influenza action of amantadine, EMBO J. 4 (1985) 3021–3024.
[9] L.H. Pinto, R.A. Lamb, The M2 proton channels of influenza A and B viruses, J. Biol. Chem. 281 (2006) 8997–9000.
[10] I. Stephenson, K.G. Nicholson, Chemotherapeutic control of influenza, J. Antimicrob. Chemother. 44 (1999) 6–10.
[11] A.S. Monto, N.H. Arden, Implications of viral resistance to amantadine in control of influenza A, Clin. Infect. Dis. 15 (1992) 362–367.
[12] A. Moscona, Neuraminidase inhibitors for influenza, N. Engl. J. Med. 353 (2005) 1363–1373.
[13] Q.M. Le, M. Kiso, K. Someya, Y.T. Sakai, T.H. Nguyen, K.H.L. Nguyen, N.D. Pham, H.H. Nguyen, S. Yamada, Y. Muramoto, T. Horimoto, A. Takada, H. Goto, T. Suzuki, Y. Suzuki, Y. Kawaoka, Avian flu: isolation of drug-resistant H5N1 virus, Nature 437 (2005) 1108.
[14] R.G. Webster, E.A. Govorkova, H5N1 influenza-continuing evolution and spread, N. Engl. J. Med. 355 (2006) 2174–2177.
[15] Centers for Disease Control and Prevention (CDC), Oseltamivir-resistant novel influenza A (H1N1) virus infection in two immunosuppressed patients – Seattle, Washington, MMWR Morb. Mortal. Wkly. Rep. (2009) 893–896.
[16] Centers for Disease Control and Prevention (CDC), Oseltamivir-resistant 2009 pandemic influenza A (H1N1) virus infection in two summer campers receiving prophylaxis – North Carolina, MMWR Morb. Mortal. Wkly. Rep. (2009) 969–972.
[17] WHO, Pandemic (H1N1) 2009 briefing note 1. Available from: <http://www.who.int/csr/disease/swineflu/notes/h1n1_antiviral_resistance_20090708/en/index.html>. (Accessed July 8, 2009).
[18] M. Yamashita, T. Tomozawa, M. Kakuta, A. Tokumitsu, H. Nasu, S. Kubo, CS-8958, a prodrug of the new neuraminidase inhibitor R-125489, Shows long-acting anti-influenza virus activity, Antimicrob. Agents Chemother. 53 (2009) 186–192.
[19] M. Kiso, S. Kubo, M. Ozawa, Q.M. Le, C.A. Nidom, M. Yamashita, Y. Kawaoka, Efficacy of the new neuraminidase inhibitor CS-8958 against H5N1 influenza viruses, PLoS Pathog. 6 (2010) e1000786.
[20] S. Kubo, T. Tomozawa, M. Kakuta, A. Tokumitsu, M. Yamashita, Laninamivir prodrug CS-8958, a long-acting neuraminidase inhibitor, shows superior anti-influenza virus activity after a single administration, Antimicrob. Agents Chemother. 54 (2010) 1256–1264.
[21] N. Sugaya, Y. Ohashi, Long-acting neuraminidase inhibitor laninamivir octanoate (CS-8958) versus oseltamivir as treatment for children with influenza virus infection, Antimicrob. Agents Chemother. 54 (2010) 2575–2582.
[22] M. Kiso, K. Shinya, M. Shimojima, R. Takano, K. Takahashi, H. Katsura, S. Kakugawa, M. Thi Quynh Le, M. Yamashita, Y. Furuta, M. Ozawa, Y. Kawaoka, Characterization of oseltamivir-resistant 2009 H1N1 pandemic influenza A viruses, PLoS Pathog. 6 (2010) e1001079.
[23] B. Isralewitz, M. Gao, K. Schulten, Steered molecular dynamics and mechanical functions of proteins, Curr. Opin. Struct. Biol. 11 (2001) 224–230;
M.S. Li, Secondary structure, mechanical stability and location of transition state of proteins, Biophys. J. 93 (2007) 2644–2654;
S. Kumar, M.S. Li, Biomolecules under mechanical force, Physics Reports 486 (2010) 1–73.
[24] F. Colizzi, R. Perozzo, L. Scapozza, M. Recanatini, A. Cavalli, Single-molecule pulling simulations can discern active from inactive enzyme inhibitors, J. Am. Chem. Soc. 132 (2010) 7361–7371.
[25] B.K. Mai, M.H. Viet, M.S. Li, Top-Leads for Swine Influenza A/H1N1 Virus Revealed by Steered Molecular Dynamics Approach, J. Chem. Inf. Model. 50 (2010) 2236–2247.
[26] A.-R. Allouche, Gabedit–A graphical user interface for computational chemistry softwares, J. Comput. Chem. 32 (2011) 174–182.
[27] W. van Gunsteren, S.R. Billeter, A.A. Eising, P.H. Hunenberger, P. Kruger, A.E. Mark, W.R.R. Scott, I.G. Tironi, Biomolecular Simulation: The GROMOS96 Manual and User Guide; Vdf Hochschulverlag AG an der ETH Zurich: Zurich, 1996.
[28] D.M.F. Aalten, R. Bywater, J.B.C. Findlay, M. Hendlich, R.W.W. Hooft, G. Vriend, PRODRG, A program for generating molecular topologies and unique molecular descriptors from coordinates of small molecules, J. Comput. Aided. Mol. Des. 10 (1996) 255–262.
[29] O. Trott, A.J. Olson, AutoDock Vina: improving the speed and accuracy of docking with a new scoring function, efficient optimization, and multithreading, J. Comput. Chem. 31 (2010) 455–461.
[30] B. Hess, C. Kutzner, D. van der Spoel, E. Lindahl, GROMACS 4: algorithms for highly efficient, load-balanced, and scalable molecular simulation, J. Chem. Theory Comput. 4 (2008) 435–447.
[31] J. Srinivasan, T.E. Cheatham, P. Cieplak, P.A. Kollman, D.A. Case, Continuumsolvent studies of the stability of DNA, RNA, and Phosphoramidate-DNA helices, J. Am. Chem. Soc. 120 (1998) 9401–9409.
[32] P.J. Collins, L.F. Haire, Y.P. Lin, J. Liu, R.J. Russell, P.A. Walker, J.J. Skehel, S.R. Martin, A.J. Hay, S.J. Gamblin, Crystal structures of oseltamivir-resistant influenza virus neuraminidase mutants, Nature 453 (2008) 1258–1261.